Ecological Informatics 77 (2023) 102218

Contents lists available at ScienceDirect

Ecological Informatics

journal homepage: www.elsevier.com/locate/ecolinf

A non-destructive approach to estimate buttress volume using 3D point cloud data

Tao Han [a], Pasi Raumonen [b], G. Arturo Sánchez-Azofeifa [a,*]

[a] Centre for Earth Observation Sciences, Department of Earth and Atmospheric Sciences, University of Alberta, T6G 2E3 Edmonton, Canada
[b] Computing Sciences, Tampere University, Korkeakoulunkatu 1, 33720 Tampere, Finland

ARTICLE INFO

Keywords:
Volume
Buttress
Alpha shape
Triangulation
Point clouds
Allometric models

ABSTRACT

Buttressed trees provide mechanical support for themselves and offer essential ecological functions, such as nutrient acquisition, while being one of the largest sources of volume or biomass estimation variation in tropical forests. In this study, we collected 51 buttressed trees from (33) Democratic Republic of Congo, (12) Indonesia, and (6) Costa Rica, including (48) point clouds, and (3) destructive measurement. Specifically, we compared the performance of the Alpha Shape Algorithm (ASA) and the Slice Triangulation (ST) method on buttress volume estimation based on 30 point clouds with two species. Six point clouds from Costa Rica were used to validate the 3D surface reconstruction method. Meanwhile, we developed three allometric models based on 36 point clouds: a diameter above the buttress-based (DAB, 39 to 203 cm) model, a diameter computed from the non-convex area ($D_{area130}$) model, and the convex hull perimeter ($D_{convex130}$) of the breast height model. The developed models were validated with independent data, including (6) point clouds and (3) destructive measurements, to highlight the broader contextualization and application of these methods. Volume estimated by the ASA and ST showed a high agreement with the reference volume acquired using the Smalian formula (relative RMSE of 0.07 and 0.11, respectively, regardless of species effect). ASA was also robust when modeling trees with more and shallower horizontal buttresses. $D_{area130}$ was the most accurate predictor to estimate buttress volume, with a lower Akaike information criterion (−66.25) than DAB (−59.55) and $D_{convex130}$ (30.56); however, DAB and $D_{area130}$ (relative RMSE of 0.21 and 0.23, respectively) showed similar performance when validated with independent datasets. Our results indicate that the ASA approach performs better than both the ST and allometric models used in this study. Furthermore, the ASA method can help correct the bias in the present and past estimates of volume and biomass of large trees, which are foundational components for understanding biomass allocation and dynamics in tropical forests contemporary fields.

1. Introduction

Buttresses are large, wide roots on all sides of a shallowly rooted tree that prevent the trees from falling (Abu Hanifa Mehedi et al., 2012; Chapman et al., 1998), and buttresses balance trees against unidirectional stresses such as asymmetrical canopies and prevailing winds (Chapman et al., 1998; Zhiyuan et al., 2013). Buttresses can act as barriers to matter flow, while also increasing the tree's contact area with the ground, resulting in higher litter accumulation, soil moisture, and nutrients (Pandey et al., 2011). Large trees are more likely to have buttresses than small trees, particularly in tropical forests (Zhiyuan et al., 2013). These large trees enhance the biodiversity of an area by providing a microenvironment where insects and other organisms can nest and seek shelter (Tang et al., 2011). Moreover, they fix large amounts of carbon because of their high wood volume, making them of interest in climate adaptation research (Nölke et al., 2015).

The occurrence of buttresses has an enormous impact on the estimation of the volume and biomass of large trees, leading to errors in the estimates of aboveground carbon in tropical forests (Nogueira et al., 2006). This error is due to the fact that measurements of diameter, basal area, and wood volume consistently treat the trunk as a cylinder, thus assuming that any cross-section of the trunk is a circle (Cushman et al., 2014). Buttressed trees pose a particular challenge in the measurement of diameter at the breast height (DBH). Many tree buttresses extend well above the standard breast height, which means trunks are not cylindrical at 1.3 m (Cushman et al., 2014). Therefore, assuming the trunk is a

* Corresponding author.
E-mail address: arturo.sanchez@ualberta.ca (G.A. Sánchez-Azofeifa).

https://doi.org/10.1016/j.ecoinf.2023.102218
Received 2 January 2023; Received in revised form 6 June 2023; Accepted 13 July 2023
Available online 17 July 2023
1574-9541/

cylinder would lead to overestimation of diameter and volume measurement in buttressed trees (Clark, 2002; Nogueira et al., 2006).

Because buttressed trees have complex structures, several methods have been developed to better estimate their volume and biomass (Cushman et al., 2021, 2014). The diameter above the buttress (DAB), where the stem reaches a relatively regular circle is one of the most widely used variables for estimating the wood volume of buttressed trees (Bauwens et al., 2017). There is no fixed definition of the height at which the DAB should be measured. Generally, moving the point of measurement up 0.30 m, or 0.50 m above the buttresses is accepted in many studies (Cushman et al., 2014; Newbery et al., 2009; Nölke et al., 2015).

Inconsistencies and uncertainties in tree volume and biomass estimations are generally due to the various methods used to measure DAB. In general, field approaches often underestimate volume and biomass because they often use a lower value than the DBH (due to tree stem diameter decreasing with height; Cushman et al., 2021). This underestimation has been accounted for by using a scale factor and the non-convex area and convex hull perimeter of buttresses at breast height (Bauwens et al., 2017; Nölke et al., 2015). Furthermore, the diameter $D_{area130}$, derived from the non-convex area of buttresses (1.3 m), has been identified as a more robust predictor of biomass than the DAB, and the diameter calculated from a circular disc with the same perimeter as the convex hull perimeter at 1.3 m ($D_{convex130}$) (Bauwens et al., 2017).

Current methods for estimating the volume and biomass of buttressed trees are labor intensive, expensive, slow, and exhibit a high degree of variability (Cushman et al., 2021; Nölke et al., 2015). These methods can be divided into destructive and non-destructive methods. Destructive methods include calculations of volume and biomass based on cross-sections of logged trees, which are dried and weighted (Dean and Roxburgh, 2006; Nogueira et al., 2006; Takoudjou et al., 2018). These approaches, which are accurate and are used to calibrate allometric models, are not often used because of their cost, instrumentation issues, and harvesting restrictions (Calders et al., 2015; Chapman et al., 1998; Zhiyuan et al., 2013).

Non-destructive approaches can be divided into three categories: 1) wire methods (Ngomanda et al., 2012), 2) convex methods (Dean and Roxburgh, 2006), and 3) terrestrial photogrammetry (TP) or laser scanning (TLS) methods (Calders et al., 2020; Cushman et al., 2021). Both the wire and convex methods produce inconsistent results and are slow because of the amount of work required to collect and process information (Bauwens et al., 2017). TP and TLS are more recent approaches used to deal with the buttress estimation problem as they can both retrieve a high-accuracy 3D point cloud (Calders et al., 2020, 2015; Cushman et al., 2021). The photogrammetric process is a cost-efficient method for measuring the 3D structure of trees, although it is easily affected by understory conditions (low vegetation and lianas, as well as poor light conditions) in the forest (Cushman et al., 2021). For example, approximately 20% of the photographs were unable to construct three-dimensional point cloud because of sub optimal acquisition (Bauwens et al., 2017). In addition, TLS can offer precise measurements of 3D tree structures and is not limited by poor light conditions; occlusion effects caused by lianas and other understory vegetation can be a problem (Moorthy et al., 2019).

With the increasing availability of point clouds, methods have been developed to convert them into volumes. For example, tree volume was calculated using the Smalian formula as cited by Nölke et al. (2015), which separates tree point clouds into several vertical slices, and then the sum volume of each slice. According to Berger et al. (2014) and Kankare et al. (2013a, 2013b), the uncertainty in estimating the true volume when using the Smalian formula was considered negligible and ignored. In addition, the Quantitative Structure Model (QSM) has been widely used to estimate tree volume in the recent years (Raumonen et al., 2013). The QSM assumes that the tree is composed of cylinders with different diameters from the ground to the crown. However, this assumption is problematic for buttressed trees. For instance, Gonzalez de Tanago et al. (2018) used QSM to estimate the biomass of buttresses based on TLS point clouds, indicating that QSM cylinders were unable to capture the detailed structure of buttresses, resulting in higher errors in the estimation of buttress volumes. Thus, a method that can handle the volume estimation of buttressed trees is needed to eliminate variations in aboveground carbon estimation.

Table 1
General description of the three databases used in this research.

Database	Acronym	Location	Methods	Number	Species
The Yangambi Reserve, Democratic Republic of Congo	YR	0° 46′ 3″ N 24° 26′ 29″ E	Photogrammetry	30	2
			Destructive	3	2
Bogor Botanical Garden, Indonesia	BBG	6° 35′ 51″ S 106° 47′ 54″ E	Terrestrial Laser Scanning	12	6
Santiago de Puriscal, Costa Rica	SP	9° 49′ 55" N 84° 19′ 60" W	Terrestrial Laser Scanning	6	6

Using a triangulation method may be a better option than cylinders to model buttresses (Disney et al., 2018). The Alpha Shape Algorithm is one of the most robust triangulation algorithms that can retain most of the original surface features (Bonneau et al., 2019; Edelsbrunner and Mücke, 1994). Although the alpha shape algorithm has been used to estimate crown attributes (Hadas et al., 2017) or canopy volume of orange groves (Colaço et al., 2017), its application to buttressed trees has not been well studied.

In this study, we address some of the knowledge gaps in buttress modeling indicated above to produce a consistent, accurate, and automated method to estimate tree buttress volume and biomass. In this study, to estimate buttress volumes, we tested two different surface reconstruction methods: the Alpha Shape Algorithm (ASA) and a Slice Triangulation (ST) algorithm for 3D point cloud surface reconstruction (Bonneau et al., 2019; Disney et al., 2018; Edelsbrunner and Mücke, 1994; Su et al., 2020). In addition, we developed allometric models for buttress volume estimation and then identified the most robust predictor to estimate buttress volume from DAB, the diameters derived from the non-convex area ($D_{area130}$), and convex hull perimeter ($D_{convex130}$) of the buttressed trees at breast height. We used buttressed trees from three databases distributed worldwide to achieve our two goals.

2. Materials and methods

2.1. Data sources

We used three databases of buttressed trees collected from different locations around the world: (1) the Yangambi Reserve (YR) from the Democratic Republic of Congo, (2) the Bogor Botanical Garden (BBG) from Indonesia, and (3) Santiago de Puriscal (SP) from Costa Rica (Table 1).

The YR database consists of 30 point clouds of buttressed trees (Trees 1 to 30 in Table S1), including two species, *Celtis mildbraedii* (*C. mildbraedii*) and *Entandophragma cylindricum* (E. cylindricum), generated using terrestrial photogrammetry (Bauwens et al., 2017). In addition, the YR database has three extra buttressed trees that were destructively measured (Table S2). The BBG database contains 12 buttressed trees (six species) generated using a multi-scan TLS method (Nölke et al., 2015). Thirty trees from the YR database were used for the alpha shape and slice triangulation reconstruction process. Of the 45 trees (DAB ranging from 39 to 203 cm) used from the YR and BBG databases, 36 trees (Table S1) containing four species were used for allometric model training, and nine (Table S2), including six species for

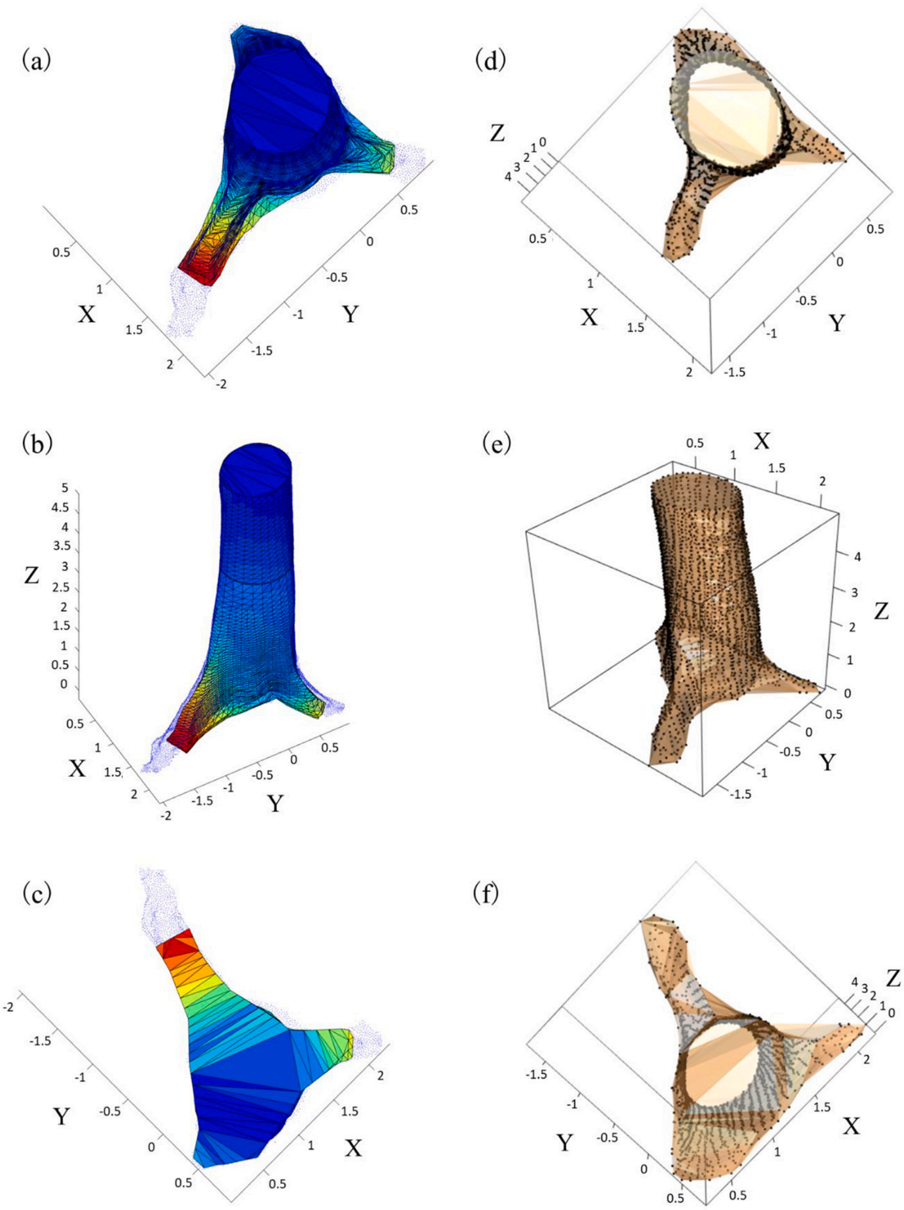

Fig. 1. Results of final buttress shape using the Alpha Shape Algorithm (ASA) and the Slice Triangulation (ST) for tree 1, (a) Top view using the ST; (b) Side view using the ST; (c) Bottom view using the ST; (d) Top view using the ASA; (e) Side view using the ASA; (f) Bottom view using the ASA.

testing. Considering the sample sizes, and overfitting problem, we applied a six-fold cross-validation strategy to the training data to assess model performance. The SP database consists of six point clouds of buttressed trees created using a multi-scan TLS method. We used these six trees to validate the alpha-shape algorithm for buttress reconstruction.

2.2. Data preprocessing

Two preprocessing steps were used to clean the point clouds. First, a statistical outlier removal (SOR, version 2.11, Cloud Compare, GPL software) filter was used to remove noisy points away from the main trunk in the Cloud Compare. The following parameters were used to run the algorithm: the number of points used for mean distance estimation (*nPoints*), and the standard deviation multiplier threshold (*nSigma*). Here, we used the default setting in Cloud Compare (*nPoints* = 6, *nSigma* = 1). Second, the point cloud was down sampled to 0.01 m to ensure uniform data distribution and improve computational efficiency (Guzmán et al., 2020).

2.3. Slice triangulation and alpha shape algorithm

Surface reconstruction algorithms aim to construct a complete surface from a 3D point cloud (Su et al., 2020). The Slice Triangulation (ST) method divides the trunk point cloud into thin equal-height horizontal cross-sections (slices) and then uses curves consisting of short line segments to reconstruct the boundary curve of these slices (Disney et al., 2018). The boundary curve reconstruction starts from the highest slice and then goes downwards for each slice at time. For each slice (other than the first slice), the vertices in the above slice are projected onto the slice to provide initial estimates of the vertices, which are then modified by the data to better fit the current slice. This also allows interpolation when occluded areas exist, as the projected vertex can then be used as such. The distance between consecutive vertices inside a slice is roughly constant; thus, if the length of the boundary curve increases sufficiently, new vertices can be created. The vertices of the curves in consecutive slices were then systemically connected to organize a uniform triangulated surface. The bottom and top planes were triangulated using Delaunay Triangulation (DT) to close the surface. The volume enclosed by triangulation is calculated using the divergence theorem, which uses the outward surface normal and area of triangles (Pfeffer, 1986).

Because the ST method uses horizontal slices, it can have two types of errors: One, if the buttress is on a sloped non-flat ground, the slices do not evenly cover the bottom of the buttress in the sense that parts of the vertices in the slice are only extrapolated from the above slice and are already below the ground level. Thus, these extrapolated vertices below ground level should not be modeling the buttress. Second, if some of the buttresses are nearly horizontal, the slices and their boundary curves fail to model them accurately, and the model usually cuts the buttresses short. Therefore, we applied a height transformation strategy to reduce these effects using the ST method. Specifically, we first flattened the ground level: The ground level model can be seen as a function G (x, y) = z, which gives the z-coordinate of the ground level for each (x, y). In addition, the lowest z-coordinate of the vertices of the ground model is z_0. Then, a point Q = (x, y, z) of the point cloud is mapped to a point Q' = (x, y, z − G (x, y) + z_0), making the transformed point cloud at ground level flat with a constant z coordinate equal to z_0. Then we applied another transformation for the bottom part of the point cloud to increase the slope of the buttresses so that they would not be so close to horizontal. The transformation is parabolic such that at the starting height it maps the points to the same location, but below that height, the points are increasingly mapped lower depending on their height. Thus, the point cloud was elongated vertically, and the elongation was stronger when the points were closer to the ground level. Note that, this transformation cannot help with truly horizontal buttresses but only when the buttresses have a downwards slope. After the transformations, we applied ST to produce a buttress triangulation model. Finally, we mapped the triangulation model back to the original coordinates and computed the buttress volume (see Fig. S1).

The Alpha Shape Algorithm (ASA) can use DT to describe the shape of a limited number of points in a set with high accuracy (Edelsbrunner and Mücke, 1994). Moreover, ASA can maintain a balance between hole-filling and loss of detail; therefore, it is often used for surface reconstruction (Bonneau et al., 2019). Concerning the ASA, the output of the final surface shape is mainly affected by parameter α (Hadas et al., 2017). α represents the refinement level for a given set of points. With a small value of α, the shape reverts to the original point sets, whereas a large value of α often indicates the shape of a convex polygon (see Gardiner et al., 2018).

To obtain an accurate buttress volume, we selected the smallest α value when a watertight manifold mesh was produced. A mesh is watertight if there are no surface holes on it (Bonneau et al., 2019), and this step can be visually inspected in R Studio (Guzmán et al., 2021). The implementation of ASA on buttress modeling was performed using the R package *rTLS* (Guzmán et al., 2021; Lafarge and Pateiro-lopez, 2017). In this package, the parameter of max.*height* in *trunk_volume* function can extract all the points in the cloud lower than a given height, which provides an efficient way to obtain the buttress volumes under the measurement height of DAB (H_{DAB}). ST was applied in MATLAB (Raumonen et al., 2013).

2.4. Scale factor

The scale factor is a commonly used metric for estimating the volume of buttresses. Here, we used the same metrics used in Bauwens et al. (2017) and Nölke et al. (2015) to define the proportion of buttress volume that is not considered when the volume is calculated as a cylinder with a diameter equal to DAB (Eq. 1):

$$f = 1 - \frac{\pi DAB^2 H_{DAB}}{4V} \tag{1}$$

where V is the estimated volume of the buttressed part of the stem (in m^3) and H_{DAB} (m) is the measurement height of the DAB. Three different volumes were calculated with V_a as the volume estimated by the alpha shape algorithm, V_t as the volume estimated by slice triangulation, and V_b as the buttress volume estimated by the Smalian formula. A two-sample *t*-test was used to determine whether there was any evidence that the mean *f* value was different between the alpha shape volume (f_a), slice triangulation volume (f_t), and the reference volume (f_b) estimated by the Smalian formula.

2.5. Volume predictors

To define the most robust predictor for volume estimation of buttressed trees, we fitted functions to describe the relationships between the reference volume and the following predictors: DAB, $D_{area130}$, and $D_{convex130}$. See Fig. 1 in Nölke et al. (2015) to determine how these three metrics were estimated from the point clouds. A log-transformation strategy was applied to meet the assumption of normality and homoscedasticity (Barbeito et al., 2017). The equation for calculating the buttress volume is shown (Eq. 2). The basis of Eq.2 is based on the volume equation of the cylinder, which means that the diameter and height information (H_{DAB} here) are required:

$$ln(V_b) = cln\left(D^2 \times H_{DAB}\right) + d \tag{2}$$

where D is one of the diameters mentioned above, c and d are the model parameters, and ln is the natural logarithm.

A correction factor (CF) was used to correct the systematic bias generated by log-transformation, when back-transforming the calculation into volume (Basuki et al., 2009; Sprugel, 1983). This equation is calculated as follows (Eq. 3):

$$CF = exp^{\left(MSE^2/2\right)} \tag{3}$$

where MSE is the mean squared error of the line fitted by the natural logarithm.

We used six-fold cross-validation to obtain a robust idea of the error of our regression model (to avoid overfitting). The final model was trained on the entire training dataset. Additionally, we used the Akaike Information Criterion (AIC) and Bayesian Information Criterion (BIC) (Atkins et al., 2022), to determine the best predictor fitted to the training data.

2.6. Validation

The absolute error of volume estimation using allometric equations is difficult to calculate without destructive harvesting methods (Cushman et al., 2021); however, the YR database includes measurements from three harvested trees, allowing for an assessment of the absolute error in the model. To illustrate the broader application of our method, we validated diameter-based models on these three harvested trees to obtain the absolute error of their volume estimates. Additionally, six TLS-measured trees were included for validation to determine whether the diameter-based models performed differently on TLS and destructively harvested trees. Detailed information regarding these nine trees is provided in Table S2.

2.7. Modeling buttresses from the SP database

Understory vegetation in dense tropical forests can obscure the target tree in point clouds even if a multi-scan strategy is applied (Calders et al., 2015). Meanwhile, buttress structures can be diverse (e.g., more well-extended and shallow buttresses) because of the effect of the local forest environment. Here, the YR database collected the point clouds of buttressed trees such that all understory vegetation and small lianas up to 2 m high around the target tree were cleared, making it a low-

Table 2
Regression analysis results of the reference volume (V_b) and V predicted by slice triangulation (V_t) and alpha shape algorithm (V_a), respectively. RMSE: root mean squared error; RRMSE: relative RMSE, refers to the RMSE divided by mean values. (., *p*-value >0.05; *, 0.05 < p-value <0.01; **, 0.01 < p-value <0.001; ***, p-value <0.001).

Method	Species	*V*	Intercept	D.f	RMSE (m^3)	Mean (V_b)	RRMSE
Alpha Shape Algorithm	E.cylindericum	***	.	15	0.50	10.06	0.05
	C. mildbraedii	***	.	11	0.32	2.12	0.15
	Both	***	*	28	0.49	6.62	0.07
Slice Triangulation	E.cylindericum	***	**	15	0.82	10.06	0.08
	C. mildbraedii	***	.	11	0.32	2.12	0.15
	Both	***	*	28	0.74	6.62	0.11

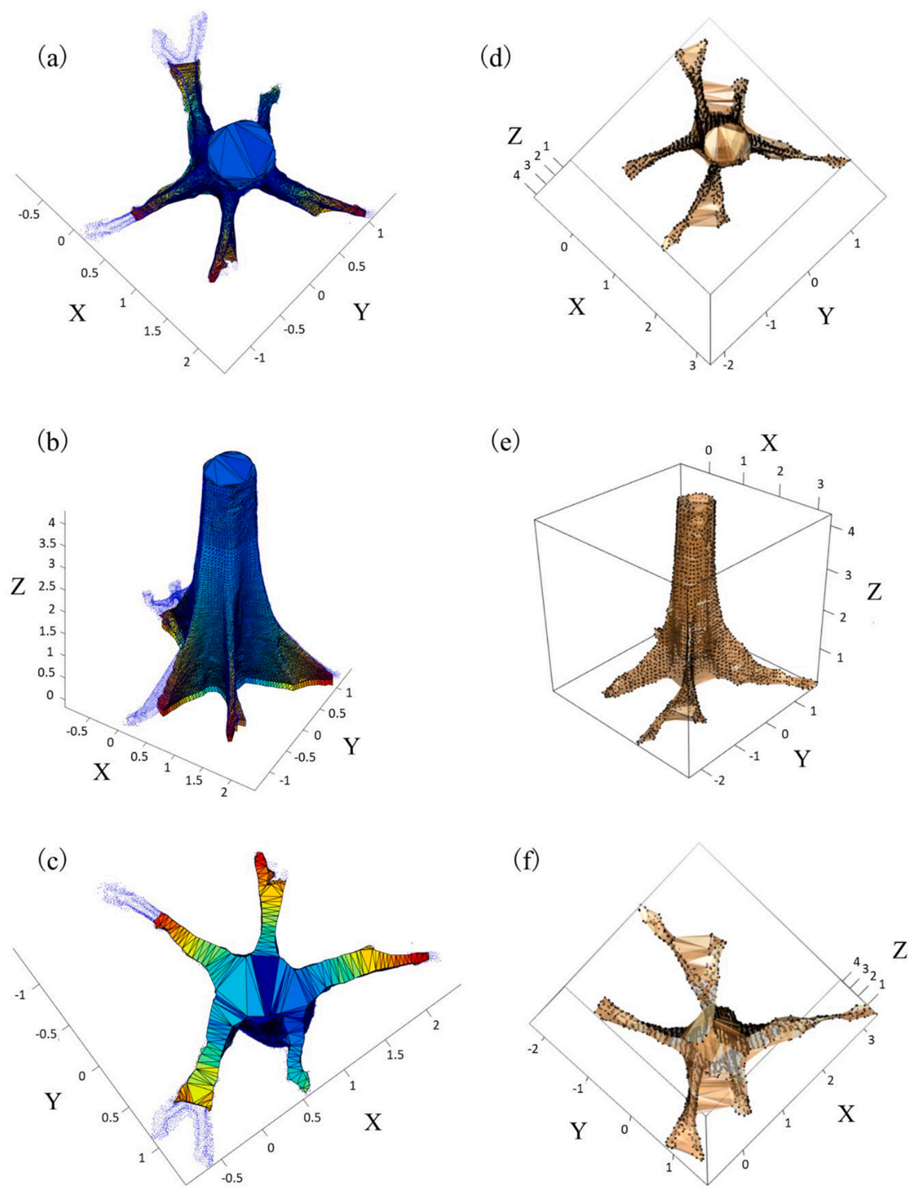

Fig. 2. Results of final buttress shape from the Alpha Shape Algorithm (ASA) and the Slice Triangulation (ST) for tree 27, (a) Top view using the ST; (b) Side view using the ST; (c) Bottom view of using the ST; (d) Top view using the ASA; (e) Side view using the ASA; (f) Bottom view using the ASA.

structural complexity control (Bauwens et al., 2017). In contrast, the SP database consisted of six buttressed trees without pre-cleaning. In addition, these trees tended to have shallow and well-extended buttresses. We used trees from the SP database to test the effectiveness of the ASA method for complex buttresses in highly obscured forests.

3. Results

3.1. Slice triangulation vs. alpha shape algorithm

Overall, we found that the ASA and ST performed similarly. The ASA tends to have a lower relative RMSE than the ST method when the volume of both species is estimated (Table 2), 0.07 versus 0.11

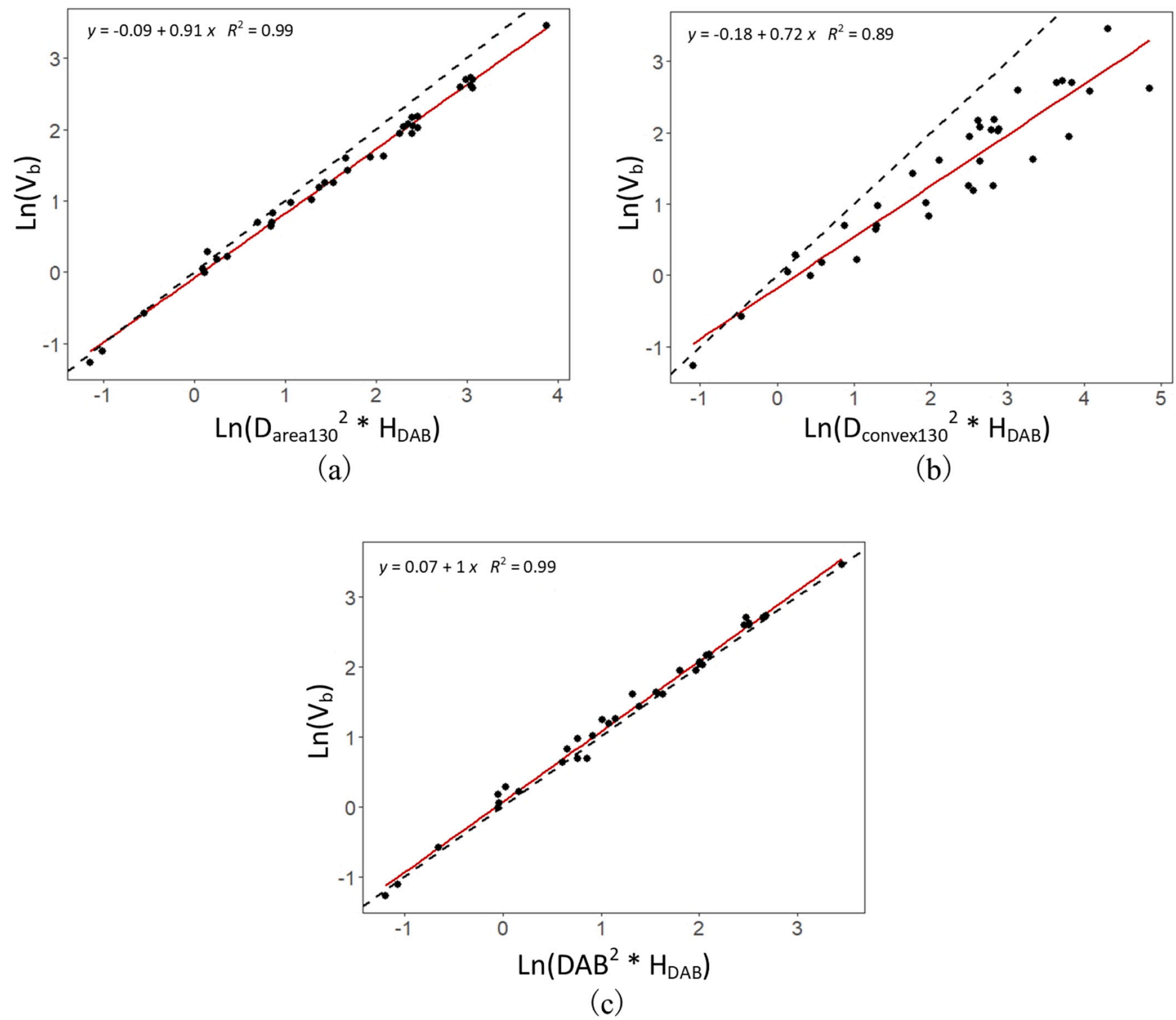

Fig. 3. (a) The relationship between $D_{area130}$ and the reference volume; (b) relationship between $D_{convex130}$ and the reference volume; (c) relationship between DAB and the reference volume. The dashed represents 1:1 identity line, and solid line is the fitted functions.

respectively. These differences were not statistically significant ($p = 0.60$). In addition, both the ASA and the ST methods generate a larger RRMSE for the *C. mildbraedii* than for the E.cylindericum (0.15 vs. 0.05 and 0.15 vs 0.08, respectively). Moreover, E.cylindericum (10.06 m^3) generated five times a larger volume than *C. mildbraedii* (2.12 m^3), while ST (0.08) produced a larger RMSE for E.cylindericum than ASA (0.05).

Figs. 1 and 2 present the modeling results using the ASA and ST approaches for Tree 1 (E.cylindericum) and Tree 27 (*C. mildbraedii*) from the YR database. The ST method cannot capture the true shape of Tree 1 (Fig. 1 a-c) and Tree 27 (Fig. 2 a-c) when the buttress is longer. In contrast, the ASA creates a better buttress model on Tree 1 (Fig. 1 d-f); however, when the tree presents more and shallower horizontal buttresses, the ASA tends to generate more overlapping areas (i.e., Tree 27; Fig. 2 d-f) leading to an overestimation of the *C. mildbraedii* volume (also see Fig. S2).

When the ASA (f_a) and ST (f_t) volumes were compared to the reference volume (f_b), there was no evidence that their mean values were different in either species (see supplementary materials; *C. mildbraedii*: f_a vs. f_b, $p = 0.11$, f_t vs. f_b, $p = 0.56$; E.cylindericum: f_a vs. f_b, $p = 0.14$, f_t vs. f_b, $p = 0.22$). However, there is strong evidence that the mean f_a differs between the two species ($p = 0.003$). In contrast, we found no evidence that the mean f_b ($p = 0.48$) or f_t (p = 0.56) differed between the two species (Fig. S3).

3.2. Volume estimation using the standard predictor

To develop a more applicable allometric model for volume estimation, we included six buttressed trees from the BBG database for model training. Therefore, we had 36 trees for model training and nine trees for validation. The six-fold cross-validation errors for the $D_{area130}$, DAB, and $D_{convex130}$ models on the training data are given in Tables S4, S5, and S6, respectively, showing that the $D_{area130}$ and DAB models fit well with the training data. Fig. 3 shows the final allometric models fitted to the entire training dataset. The allometric models developed with either $D_{area130}$ or DAB presented an identical R^2 value of 0.99, whereas the value for $D_{convex130}$ was 0.89.

Of the three models fitted to the 36 buttressed trees, the model derived from $D_{area130}$ provided the best fit with the lowest Akaike

Table 3
Results of the regression analysis for the volume estimation equations (Eqn. 2). D.f. = degrees of freedom; AIC = Akaike Information Criterion; BIC = Bayesian Information Criterion; RMSE = Root Mean Squared Error after back transforming the results, refers to volume error (m^3); RRMSE = relative RMSE. (., p-value >0.05; **, 0.01 < p-value <0.001; ***, p-value <0.001).

Predictor	D^2	Intercept	D.f.	AIC	BIC	RMSE	RRMSE
$D_{area130}$	***	**	34	−66.25	−61.50	0.52	0.08
$D_{convex130}$	***	.	33	30.56	35.22	3.92	0.60
DAB	***	**	34	−59.55	−54.79	0.67	0.11

Table 4
The validation results of different models on six TLS trees and three harvested trees; the results from the harvested trees are italicized. TLS = Terrestrial Laser Scanning; V_p = predicted values of volume; RE = |relative error|; $RRMSE_{TLS}$ = relative RMSE of TLS trees; $RRMSE_{Des}$ = relative RMSE of destructively harvested trees.

No.	V_b (m^3)	$D_{area130}$		$D_{convex130}$		DAB	
		V_p (m^3)	RE	V_p (m^3)	RE	V_p (m^3)	RE
T1-BBG	7.45	5.68	0.24	4.09	0.45	5.17	0.31
T2-BBG	7.97	9.67	0.21	15.78	0.98	5.91	0.26
T3-BBG	2.67	2.76	0.03	3.19	0.19	2.86	0.07
T4-BBG	20.5	19.28	0.06	19.66	0.04	21.64	0.06
T5-BBG	17.41	20.98	0.21	31.89	0.83	13.75	0.21
T6-BBG	1.72	1.70	0.01	1.67	0.03	1.70	0.01
T1-YR	*3.07*	*3.50*	*0.14*	*5.11*	*0.66*	*3.69*	*0.20*
T2-YR	*1.27*	*1.73*	*0.36*	*2.28*	*0.80*	*1.16*	*0.09*
T3-YR	*1.66*	*2.00*	*0.20*	*2.84*	*0.71*	*1.83*	*0.11*
RRMSE		0.21		0.80		0.23	
$RRMSE_{TLS}$		0.19		0.71		0.21	
$RRMSE_{Des}$		*0.21*		*0.74*		*0.19*	

Information Criterion (AIC, −66.25) and Bayesian information criterion (BIC, −61.50) (Table 3). The RRMSE of the DAB model (0.11) was similar to that of the $D_{area130}$ model (0.08). In addition, we found no systematic overestimation or under-estimation of the volume estimates given by the DAB model (a slope coefficient of 1) from Fig. 3(c). The $D_{area130}$ model is more likely to overestimate the volume with a slope of 0.91. $D_{convex130}$ may not be a good predictor for volume estimation because it generated the highest RMSE and RRMSE.

3.3. The allometric model validation

We evaluated the performance of the diameter-based models on three destructively harvested trees and six trees scanned with TLS from the YR and BBG databases. Overall, the DAB (0.21) and $D_{area130}$ (0.23) models generated similar RRMSEs on the validation data, which outperformed the $D_{convex130}$ model in estimating volume (RRMSE = 0.80) (Table 4). Moreover, the three models built with different diameters showed similar performance on destructively sampled data and TLS data. For the TLS trees, T1-BBG generated the highest relative error among the six trees in the $D_{area130}$ (0.24) and DAB (0.31) models. In contrast, the $D_{convex130}$ and DAB models provided the best fit for T6-BBG, with the lowest buttress volumes (1.72 m^3) of all six trees. The overall RRMSE of the TLS trees in the $D_{area130}$ model (0.19) was slightly lower than that of the DAB model (0.21). In terms of the harvested trees, the relative error of $D_{area130}$ model on all trees was larger than DAB model, except for *T1-YR* (0.14 vs. 0.20). In addition, the DAB and $D_{area130}$ models showed similar RRMSE (0.21 vs. 0.19). Finally, f_b (Eq. 1) of the 45 trees from YR and BBG databases was 0.28 (±0.09), meaning that the cylindrical volume calculated from DAB underestimated 28% of all 45 buttress volumes.

Fig. 4 shows two examples of buttressed trees from the SP database. Compared with tree 27 in Fig. 2, the trees in Fig. 4 had more and shallower horizontal buttresses. Visual inspection of Fig. 4 indicates that the ASA can capture all buttresses, although the ASA tends to generate some overlapping areas when the neighboring buttresses are close.

4. Discussion

In this study, we tested the performance of the Alpha Shape Algorithm (ASA) and Slice Triangulation (ST) in estimating buttress volume. Overall, the ASA and ST methods tended to have better volume estimations than the allometric models. We also demonstrate that ASA is a more applicable method than ST for buttress volume estimation.

4.1. The alpha shape algorithm vs. slice triangulation

Large trees exhibit higher variability in volume and biomass estimates, especially in tropical areas, where the trees show considerable stem irregularities, such as buttressed trees (Nölke et al., 2015). The problems in estimating volume and biomass posed by buttressed trees have been widely reported but are poorly understood (Cushman et al., 2021, 2014). To eliminate this bias, Gonzalez de Tanago et al. (2018) used QSM cylinders to reconstruct tropical trees, including small (DBH ≤ 70 cm) and large trees (DBH > 70 cm), where the latter always had buttresses. The QSM approach showed a high agreement with the reference data for small trees, whereas it showed higher residuals in large trees. Our study has improved on previous methodologies by showing that ASA and ST perform similarly on volume estimation, and ASA is a more applicable and transferable method than ST. Although ASA has been shown to be robust in canopy architecture reconstruction (Colaço et al., 2017; Hadas et al., 2017), we do not see many studies using ASA to model buttresses.

It should be noted that the ASA method tends to overestimate the buttress volume when the tree presents more and shallower horizontal buttresses (Fig. 2d and Fig. S2). However, ASA can capture the true shape given the lower and wider buttresses (Fig. 1d). This is why the mean f_a is statistically different between *C. mildbraedii* and E.cylindericum. The ST method could not capture the true shape of longer horizontal buttresses (Figs. 1a and 2a). Therefore, with a larger volume in E. cylindericum trees, the ST creates a larger error than the ASA. Furthermore, the buttress structure can be very complex because of the effect of local forest environments. The trees from the SP database provide six examples of how buttresses are usually found in tropical forests. Even though the ASA tends to generate many overlapping areas between the neighboring buttresses (Fig. 4), it provides a solution effectively to estimate the volume of the buttressed trees.

4.2. Volume estimated by the diameter-based allometric models

In terms of diameter-based allometric models for volume estimation, our study indicated that the $D_{area130}$ model had the lowest AIC. This finding was similar to that of Bauwens et al. (2017), who demonstrated that the biomass allometric model with $D_{area130}$ had the lowest AIC, compared to DAB and $D_{convex130}$. However, no independent data were available by Bauwens et al. (2017) to assess the performance of the trained model. Concerning the testing process in this study, DAB and $D_{area130}$ showed similar performance, and more buttressed trees may be needed to determine a more robust predictor for volume estimates. Although there are a limited number of buttressed trees that are scanned with TLS and destructively harvested trees for validation, the similar performance of allometric models on them do give indicates that TLS is a reliable alternative method for destructive measurement without loss of accuracy, as supported by Calders et al. (2015, 2020) and Disney et al. (2018).

Allometric models have been widely used for volume or biomass estimation in forestry, but large trees are often underrepresented in the calibration of such models (Clark and Kellner, 2012; Newnham et al., 2015). The utilization of tree metrics such as DAB or a scale factor (*f* index here) is recommended to estimate buttress volume (Ngomanda et al., 2012; Nölke et al., 2015). In this study, not only we built

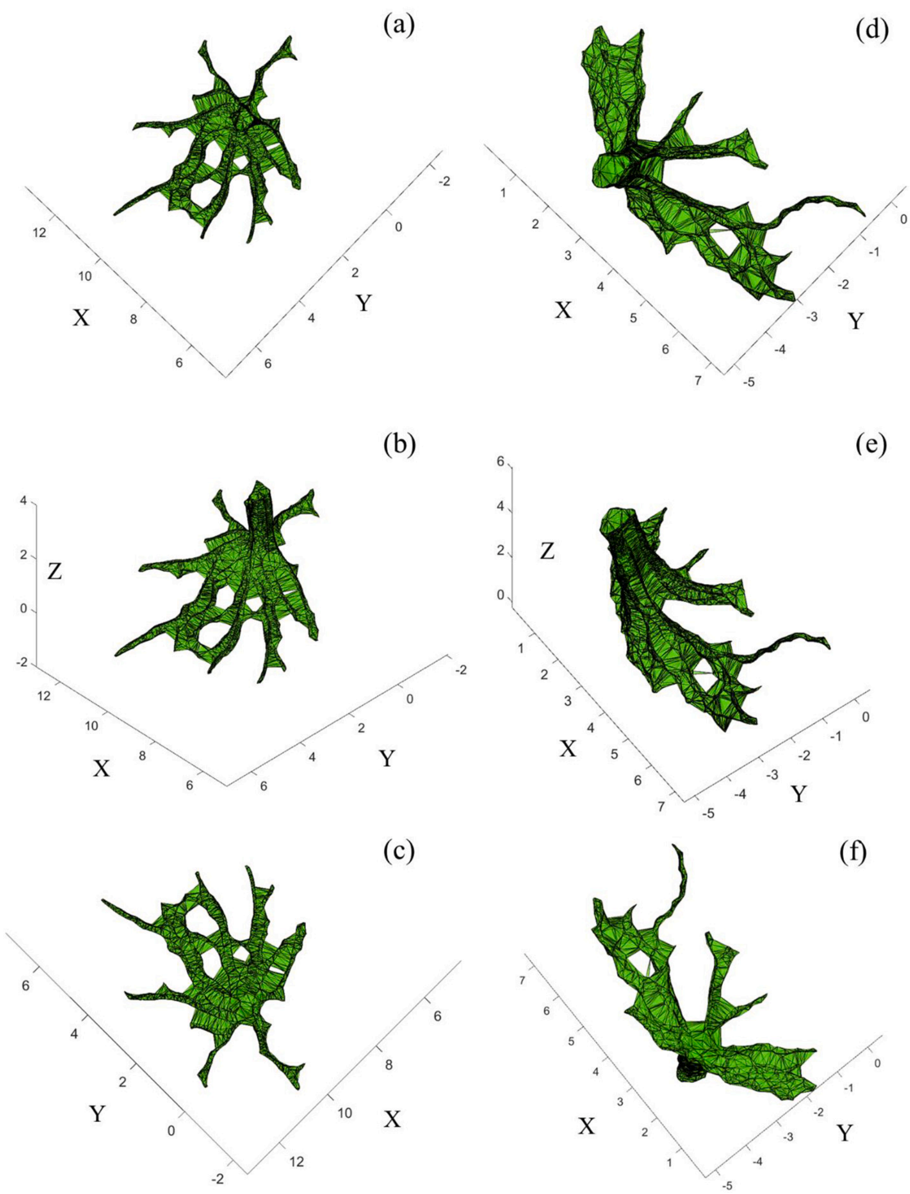

Fig. 4. The predictions of alpha shape algorithm (ASA) on trees from the Santiago de Puriscal, Costa Rica (SP database): (a) Top view of Tree 1 from the SP database; (b) Side view of Tree 1 from the SP database; (c) Bottom view of Tree 1 from the SP database; (d) Top view of Tree 2 from the SP database; (e) Side view of Tree 2 from the SP database; (f) Bottom view of Tree 2 from the SP database.

allometric models with DAB and the diameter derived from the non-convex area and convex hull perimeter of buttressed trees at breast height, but we also calculated the scale factor, which is the proportion of the underestimation of buttress volume, when DAB was used for cylindrical volume modeling. The RRMSE of the DAB or $D_{area130}$ based model in this study ranged from 0.21 to 0.23 on independent data. Because we only used nine buttressed trees for validation, we expect more studies in the future to assess the performance of our proposed allometric models. The mean f_b (0.28 ± 0.09) of all 45 trees indicated that approximately 28% of buttress volume was not considered when the volume was estimated with DAB. This value was similar to that reported by Bauwens et al. (2017) (0.26), and lower than that reported by Nölke et al. (2015) (0.35).

It should be mentioned that we did not include the harmonized tree diameter (equivalent diameter at breast height estimated by taper models) to estimate buttress volume due to the limited sample sizes and the amount of work. The harmonized diameter can reduce bias in biomass estimation owning to the nonstandard diameter (the different height of the point of measurement) (Cushman et al., 2021). For example, recent studies by Bauwens et al. (2021) revealed that harmonized tree diameter can reduce biomass underestimation (up to 15% at the plot-level) for irregular trees using allometric models. With the increase in 3D tree data available from laser scanning or photogrammetry, future research could focus on the improvement of trunk taper models to estimate harmonized tree diameter.

4.3. The utilization of 3D point cloud data

Compared to the ASA and ST methods, volume estimation using allometric models may not be a reliable indicator of volume for buttressed trees. The ASA and ST methods generated lower RRMSEs (0.07 and 0.11, respectively) than the allometric models (0.21 for $D_{area130}$; 0.23 for DAB, respectively) on validation data. Similar issues were addressed by Calders et al. (2015), Kankare et al. (2013a), and Lau et al. (2019). For example, Calders et al. (2015) identified that biomass estimates from the 3D point cloud using the QSM reconstruction approach showed a higher agreement (concordance correlation coefficient (CCC) of 0.98) with the reference data than the allometric models (CCC = 0.68–0.78). Utilizing TLS or terrestrial photogrammetry provides new insights into how to measure tree structures in a detailed 3D view (Calders et al., 2020). Consequently, irregularly large trees, such as buttressed trees, can also be modeled with higher accuracy. Because the ASA tends to overestimate the buttressed tree volume when the trees present more and shallower horizontal buttresses, more robust and automatic tree construction methods are expected with the increasing availability of 3D point clouds. More advanced surface reconstruction methods that can eliminate the weakness of slice triangulation (missing longer buttresses) and alpha shape algorithm (overestimation) are expected.

5. Conclusions

In this study, we used the Alpha Shape Algorithm and the Slice Triangulation method to estimate the buttress volume based on 3D point clouds to reduce the variation between allometry and the true volume. The volume estimates of the alpha shape algorithm and slice triangulation method shows a similar RRMSE, with both methods outperforming allometric models developed with DAB and $D_{area130}$. Meanwhile, the alpha shape algorithm tends to perform better than slice triangulation when the trees present more and shallower horizontal buttresses. With databases including trees from three continents, this model can be applied to tropical buttressed trees globally, increasing its applicability to industry and field research. Additionally, large trees have been underrepresented in previous studies, providing an opportunity for the method presented here to better capture the comprehensive values of volume and biomass, and improve carbon storage estimations in tropical forests.

CRediT authorship contribution statement

Tao Han: Conceptualization, Methodology, Investigation, Writing – original draft. **Pasi Raumonen:** Methodology, Writing – review & editing. **G. Arturo Sánchez-Azofeifa:** Supervision, Writing – review & editing.

Declaration of Competing Interest

The authors have declared that no competing interests exist.

Data availability

The TLS data collected by the authors are available from the Tropi-Dry Dataverse repository. The YR database is available at (http://hdl.handle.net/2268/202113), and the BBG database does not provide point clouds but provides detailed information for each tree.

Acknowledgements

This research was funded by National Science and Engineering Research Council of Canada (NSERC) Discovery Grant. This research was also supported by the Academy of Finland's Center of Excellence of Inverse Modelling and Imaging. We thank Bauwens et al. (2017) and Nölke et al. (2015) for sharing data. We also thank Kalya Stan for proofreading this manuscript.

Appendix A. Supplementary data

Supplementary data to this article can be found online at https://doi.org/10.1016/j.ecoinf.2023.102218.

References

Abu Hanifa Mehedi, M., Kundu, C., Qumruzzaman Chowdhury, M., 2012. Patterns of tree buttressing at Lawachara National Park, Bangladesh. J. For. Res. 23, 461–466. https://doi.org/10.1007/s11676-012-0285-x.

Atkins, J.W., Stovall, A.E.L., Alberto Silva, C., 2022. Open-source tools in R for forestry and forest ecology. For. Ecol. Manag. 503, 119813 https://doi.org/10.1016/j.foreco.2021.119813.

Barbeito, I., Dassot, M., Bayer, D., Collet, C., Drössler, L., Löf, M., del Rio, M., Ruiz-Peinado, R., Forrester, D.I., Bravo-Oviedo, A., Pretzsch, H., 2017. Terrestrial laser scanning reveals differences in crown structure of Fagus sylvatica in mixed vs. pure European forests. For. Ecol. Manag. 405, 381–390. https://doi.org/10.1016/j.foreco.2017.09.043.

Basuki, T.M., van Laake, P.E., Skidmore, A.K., Hussin, Y.A., 2009. Allometric equations for estimating the above-ground biomass in tropical lowland dipterocarp forests. For. Ecol. Manag. 257, 1684–1694. https://doi.org/10.1016/j.foreco.2009.01.027.

Bauwens, S., Fayolle, A., Gourlet-Fleury, S., Ndjele, L.M., Mengal, C., Lejeune, P., 2017. Terrestrial photogrammetry: a non-destructive method for modelling irregularly shaped tropical tree trunks. Methods Ecol. Evol. 8, 460–471. https://doi.org/10.1111/2041-210X.12670.

Bauwens, S., Ploton, P., Fayolle, A., Ligot, G., Loumeto, J.J., Lejeune, P., Gourlet-Fleury, S., 2021. A 3D approach to model the taper of irregular tree stems: making plots biomass estimates comparable in tropical forests. Ecol. Appl. 31, 0–2. https://doi.org/10.1002/eap.2451.

Berger, A., Gschwantner, T., McRoberts, R.E., Schadauer, K., 2014. Effects of measurement errors on individual tree stem volume estimates for the Austrian national forest inventory. For. Sci. 60, 14–24. https://doi.org/10.5849/forsci.12-164.

Bonneau, D., DiFrancesco, P.-M., Hutchinson, D.J., 2019. Surface reconstruction for three-dimensional Rockfall volumetric analysis. ISPRS Int. J. Geo-Inf. 8, 548. https://doi.org/10.3390/ijgi8120548.

Calders, K., Newnham, G., Burt, A., Murphy, S., Raumonen, P., Herold, M., Culvenor, D., Avitabile, V., Disney, M., Armston, J., Kaasalainen, M., 2015. Nondestructive estimates of above-ground biomass using terrestrial laser scanning. Methods Ecol. Evol. 6, 198–208. https://doi.org/10.1111/2041-210X.12301.

Calders, K., Adams, J., Armston, J., Bartholomeus, H., Bauwens, S., Bentley, L.P., Chave, J., Danson, F.M., Demol, M., Disney, M., Gaulton, R., Krishna Moorthy, S.M., Levick, S.R., Saarinen, N., Schaaf, C., Stovall, A., Terryn, L., Wilkes, P., Verbeeck, H., 2020. Terrestrial laser scanning in forest ecology: expanding the horizon. Remote Sens. Environ. 251, 112102 https://doi.org/10.1016/j.rse.2020.112102.

Chapman, C.A., Kaufman, L., Chapman, L.J., 1998. Buttress formation and directional stress experienced during critical phases of tree development. J. Trop. Ecol. 14, 341–349. https://doi.org/10.1017/S0266467498000261.

Clark, D.A., 2002. Are tropical forests an important carbon sink? Reanalysis of the long-term plot data. Ecol. Appl. 12, 3–7. https://doi.org/10.1890/1051-0761(2002)012[0003:ATFAIC]2.0.CO;2.

Clark, D.B., Kellner, J.R., 2012. Tropical forest biomass estimation and the fallacy of misplaced concreteness. J. Veg. Sci. 23, 1191–1196. https://doi.org/10.1111/j.1654-1103.2012.01471.x.

Colaço, A.F., Trevisan, R.G., Molin, J.P., Rosell-Polo, J.R., Escolà, A., 2017. A method to obtain orange crop geometry information using a mobile terrestrial laser scanner and 3D modeling. Remote Sens. 9, 10–13. https://doi.org/10.3390/rs9080763.

Cushman, K.C., Muller-Landau, H.C., Condit, R.S., Hubbell, S.P., 2014. Improving estimates of biomass change in buttressed trees using tree taper models. Methods Ecol. Evol. 5, 573–582. https://doi.org/10.1111/2041-210X.12187.

Cushman, K.C., Bunyavejchewin, S., Cárdenas, D., Condit, R., Davies, S.J., Duque, Á., Hubbell, S.P., Kiratiprayoon, S., Lum, S.K.Y., Muller-Landau, H.C., 2021. Variation in trunk taper of buttressed trees within and among five lowland tropical forests. Biotropica 53, 1442–1453. https://doi.org/10.1111/btp.12994.

Dean, C., Roxburgh, S.H., 2006. Improving visualisation of mature, high-carbon-sequestering forests. For. Biometry. Model. Inf. Sci. 2006, 48–69.

Disney, M.I., Boni Vicari, M., Burt, A., Calders, K., Lewis, S.L., Raumonen, P., Wilkes, P., 2018. Weighing trees with lasers: advances, challenges and opportunities. Interface Focus 8, 20170048. https://doi.org/10.1098/rsfs.2017.0048.

Edelsbrunner, H., Mücke, E.P., 1994. Three-dimensional alpha shapes. ACM Trans. Graph. 13, 43–72. https://doi.org/10.1145/174462.156635.

Gardiner, J.D., Behnsen, J., Brassey, C.A., 2018. Alpha shapes: determining 3D shape complexity across morphologically diverse structures. BMC Evol. Biol. 18, 1–16. https://doi.org/10.1186/s12862-018-1305-z.

Gonzalez de Tanago, J., Lau, A., Bartholomeus, H., Herold, M., Avitabile, V., Raumonen, P., Martius, C., Goodman, R.C., Disney, M., Manuri, S., Burt, A., Calders, K., 2018. Estimation of above-ground biomass of large tropical trees with terrestrial LiDAR. Methods Ecol. Evol. 9, 223–234. https://doi.org/10.1111/2041-210X.12904.

Guzmán, Q., J.A, Sharp, I., Alencastro, F., Sánchez-Azofeifa, G.A., 2020. On the relationship of fractal geometry and tree–stand metrics on point clouds derived from terrestrial laser scanning. Methods Ecol. Evol. 11, 1309–1318. https://doi.org/10.1111/2041-210X.13437.

Guzmán, Q., J.A, Hernandez, R., Sanchez-Azofeifa, A., 2021. rTLS: Tools to Process Point Clouds Derived from Terrestrial Laser Scanning. https://CRAN.R-project.org/package=rTLS.

Hadas, E., Borkowski, A., Estornell, J., Tymkow, P., 2017. Automatic estimation of olive tree dendrometric parameters based on airborne laser scanning data using alpha-shape and principal component analysis. GISci. Remote Sens. 54, 898–917. https://doi.org/10.1080/15481603.2017.1351148.

Kankare, V., Holopainen, M., Vastaranta, M., Puttonen, E., Yu, X., Hyyppä, J., Vaaja, M., Hyyppä, H., Alho, P., 2013a. Individual tree biomass estimation using terrestrial laser scanning. ISPRS J. Photogramm. Remote Sens. 75, 64–75. https://doi.org/10.1016/j.isprsjprs.2012.10.003.

Kankare, V., Vastaranta, M., Holopainen, M., Räty, M., Yu, X., Hyyppä, J., Hyyppä, H., Alho, P., Viitala, R., 2013b. Retrieval of forest aboveground biomass and stem volume with airborne scanning LiDAR. Remote Sens. 5, 2257–2274. https://doi.org/10.3390/rs5052257.

Lafarge, A.T., Pateiro-lopez, B., 2017. alphashape3d: implementation of the 3D alpha-shape for the reconstruction of 3D sets from a point cloud. In: R Packag. Version 1.3, pp. 1–12.

Lau, A., Calders, K., Bartholomeus, H., Martius, C., Raumonen, P., Herold, M., Vicari, M., Sukhdeo, H., Singh, J., Goodman, R.C., 2019. Tree biomass equations from terrestrial LiDAR: A case study in Guyana. Forests 10, 1–18. https://doi.org/10.3390/f10060527.

Moorthy, S.M., Bao, Y., Calders, K., Schnitzer, S.A., Verbeeck, H., 2019. Semi-automatic extraction of liana stems from terrestrial LiDAR point clouds of tropical rainforests. ISPRS J. Photogramm. Remote Sens. 154, 114–126. https://doi.org/10.1016/j.isprsjprs.2019.05.011.

Newbery, D.M., Schwan, S., Chuyong, G.B., Van Der Burgt, X.M., 2009. Buttress form of the central African rain forest tree Microberlinia bisulcata, and its possible role in nutrient acquisition. Trees - Struct. Funct. 23, 219–234. https://doi.org/10.1007/s00468-008-0270-3.

Newnham, G.J., Armston, J.D., Calders, K., Disney, M.I., Lovell, J.L., Schaaf, C.B., Strahler, A.H., Mark Danson, F., 2015. Terrestrial laser scanning for plot-scale forest measurement. Curr. For. Rep. 1, 239–251. https://doi.org/10.1007/s40725-015-0025-5.

Ngomanda, A., Mavouroulou, Q.M., Obiang, N.L.E., Iponga, D.M., Mavoungou, J.F., Lépengué, N., Picard, N., Mbatchi, B., 2012. Derivation of diameter measurements for buttressed trees, an example from Gabon. J. Trop. Ecol. 28, 299–302. https://doi.org/10.1017/S0266467412000144.

Nogueira, M.A., Diaz, G., Andrioli, W., Falconi, F.A., Stangarlin, J.R., 2006. Volume and biomass of trees in Central Amazonia: influence of irregularly shaped and hollow trunks Euler. Braz. J. Microbiol. 37, 14–16. https://doi.org/10.1016/j.foreco.2006.02.004.

Nölke, N., Fehrmann, L., Nengah S, I., Tiryana, T., Seidel, D., Kleinn, C., 2015. On the geometry and allometry of big-buttressed trees - a challenge for forest monitoring: new insights from 3D-modeling with terrestrial laser scanning. iForest - Biogeosci. For. 8, 574–581. https://doi.org/10.3832/ifor1449-007.

Pandey, C.B., Singh, L., Singh, S.K., 2011. Buttresses induced habitat heterogeneity increases nitrogen availability in tropical rainforests. For. Ecol. Manag. 262, 1679–1685. https://doi.org/10.1016/j.foreco.2011.07.019.

Pfeffer, W.F., 1986. The divergence theorem. Trans. Am. Math. Soc. 295, 665. https://doi.org/10.2307/2000057.

Raumonen, P., Kaasalainen, M., Markku, Å., Kaasalainen, S., Kaartinen, H., Vastaranta, M., Holopainen, M., Disney, M., Lewis, P., 2013. Fast automatic precision tree models from terrestrial laser scanner data. Remote Sens. 5, 491–520. https://doi.org/10.3390/rs5020491.

Sprugel, D.G., 1983. Correcting for Bias in log-transformed Allometric equations. Ecology 64, 209–210. https://doi.org/10.2307/1937343.

Su, T., Wang, W., Liu, H., Liu, Z., Li, X., Jia, Z., Zhou, L., Song, Z., Ding, M., Cui, A., 2020. An adaptive and rapid 3D Delaunay triangulation for randomly distributed point cloud data. Vis. Comput. https://doi.org/10.1007/s00371-020-02011-3.

Takoudjou, S.M., Ploton, P., Sonké, B., Hackenberg, J., Griffon, S., de Coligny, F., Kamdem, N.G., Libalah, M., Mofack, G., Le Moguédec, G., Pélissier, R., Barbier, N., 2018. Using terrestrial laser scanning data to estimate large tropical trees biomass and calibrate allometric models: A comparison with traditional destructive approach. Methods Ecol Evol 9, 905–916. https://doi.org/10.1111/2041-210X.12933.

Tang, Y., Yang, X., Cao, M., Baskin, C.C., Baskin, J.M., 2011. Buttress trees elevate soil heterogeneity and regulate seedling diversity in a tropical rainforest. Plant Soil 338, 301–309. https://doi.org/10.1007/s11104-010-0546-4.

Zhiyuan, H., Yong, T., Xiaobao, D., Min, C., 2013. Buttress trees in a 20-hectare tropical dipterocarp rainforest in Xishuangbanna, SW China. J. Plant Ecol. 6, 187–192. https://doi.org/10.1093/jpe/rts031.